

Observation of Plasma Response after Hydrocarbon Pellet Injection in CHS

SHIRAI Yoshiaki^{1*}, MORITA Shigeru, GOTO Motoshi, IDEI Hiroshi, INOUE Noriyuki,
KUBO Shin, MATSUOKA Keisuke, MINAMI Takashi, OHDACHI Satoshi,
OKAMURA Shoichi, OSAKABE Masaki, SAKAMOTO Ryuichi, TAKAGI Syoji²,
TANAKA Kenji, TOI Kazuo, YOSHIMURA Yasuo and the CHS group
National Institute for Fusion Science, Toki 509-5292, Japan

¹*The Graduate University for Advanced Studies, Toki 509-5292, Japan*

²*Department of Energy Engineering Science, Nagoya Univ., Nagoya 464-8602, Japan*

(Received: 30 September 1997/Accepted: 16 February 1998)

Abstract

Results are described on NBI and ECH plasma response after hydrocarbon pellet injection in CHS. The hydrocarbon pellet injection indicated that the stored energy of the NBI discharge successfully increased for the pellet diameter of smaller than 0.32 mm, although other discharges with larger diameter of the pellet collapsed with a rapid density rise and a large increment of radiation loss.

After the pellet injection the density profiles largely changed from flat and hollow profiles to peaked profiles for both cases of the NBI and ECH plasmas. These peaked profiles were maintained until the end of the heating pulse, whereas the edge density decreases. A radial position where the pellet penetrated and a fueling efficiency are also obtained with the pellet size and the target density.

Keywords:

CHS, impurity pellet, plasma response, ablation, radiation loss, collapse

1. Introduction

A study of the particle transport characteristics is important for understanding a mechanism on the formation of the electron density profile and the plasma-wall interaction, which is a critical issue in Large Helical Device (LHD) with a well-defined divertor structure [1]. Until now this investigation has been experimentally done using gas puffing and laser blow off techniques. These methods, however, do not quantitatively give any exact results on the injected particle number. In the case of LHD, a distance from a diagnostic port to the plasma edge is nearly 4 m. There are the divertor legs between the diagnostic ports and the main plasma, and thick ergodic layer exists at the plasma edge. The tracer particle from the laser blow off can not enter the main plasma. Therefore, the application of such

methods is not adequate in LHD. The impurity pellet is considered as a powerful tool to investigate the particle transport [2]. Then, we are now preparing the impurity pellet injector for the LHD diagnostics. As a first step, the pellet experiment has been done in CHS using a prototype injector. In order to demonstrate that the impurity pellet is enough applicable to the study of the plasma particle transport, we study the plasma response after impurity pellet injection in NBI and ECH plasmas [3].

2. Experimental Setup

The pellets used in this experiment are spheres of hydrocarbon (di-vinyl-benzene polystyrene), with a diameter of 0.23–0.46 mm. The spherical pellet is

*Corresponding author's e-mail: shirai@nifs.ac.jp

accelerated by a pressurized gas gun. The velocity of the pellet is 400–500 m/s. The helium pressure as a propellant gas is about 25 atm and the pressurized helium gas is evacuated by a three-stage differential pumping system. The radial position of pellet penetration and the ablation along the pellet trajectory in the plasma are directly measured using an 11 channel visible fan array with an interference filter of CI ($\lambda_0 = 538$ nm, $\Delta\lambda_{1/2} = 2$ nm).

3. Experimental Results

In case of CHS ($V_p \sim 0.8$ m³), it is found that the NBI plasma collapses completely by hydrocarbon pellet

with a diameter larger than 0.39 mm. Then, the plasma response was examined using hydrocarbon pellets with a diameter of 0.27–0.39 mm. Figure 1 shows a typical example of the temporal evolution of the plasma stored energy in the NBI plasma ($P_{\text{NBI}} = 900$ kW, $\bar{n}_e = 3 \times 10^{19}$ m⁻³). Here, we can see that the stored energy successfully increases for small-size pellets. The radiation collapse occurs for the pellet with 0.39 mm diameter. The relation between the density rise and size of the pellet is examined. The result is shown in Fig. 2. The increment of the volume-integrated density (ΔN_e -exp) calculated from the observed $n_e(r)$ is plotted against the total number of electrons of the injected hydrocarbon pellet (ΔN_e -cal). In the calculation it is

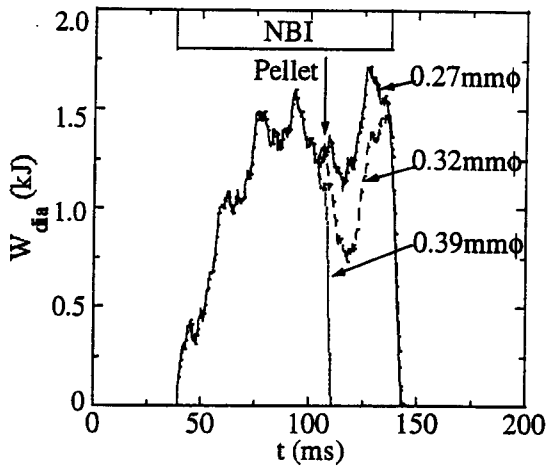


Fig. 1 Time evolution of plasma stored energy with hydrocarbon pellet injection in the NBI plasma ($P_{\text{NBI}} = 900$ kW, $\bar{n}_e = 3 \times 10^{19}$ m⁻³).

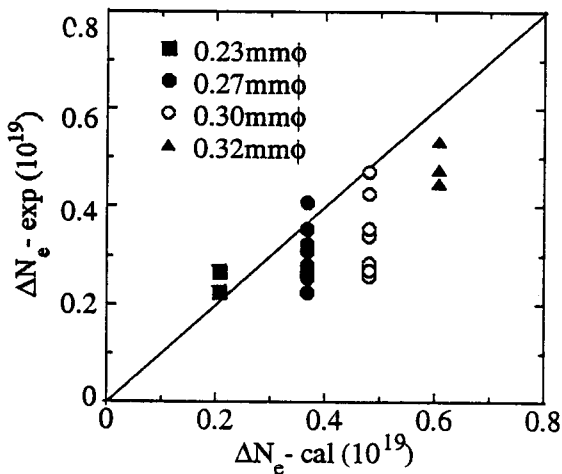


Fig. 2 Increment of volume-integrated electron density against electron number of the injected pellet.

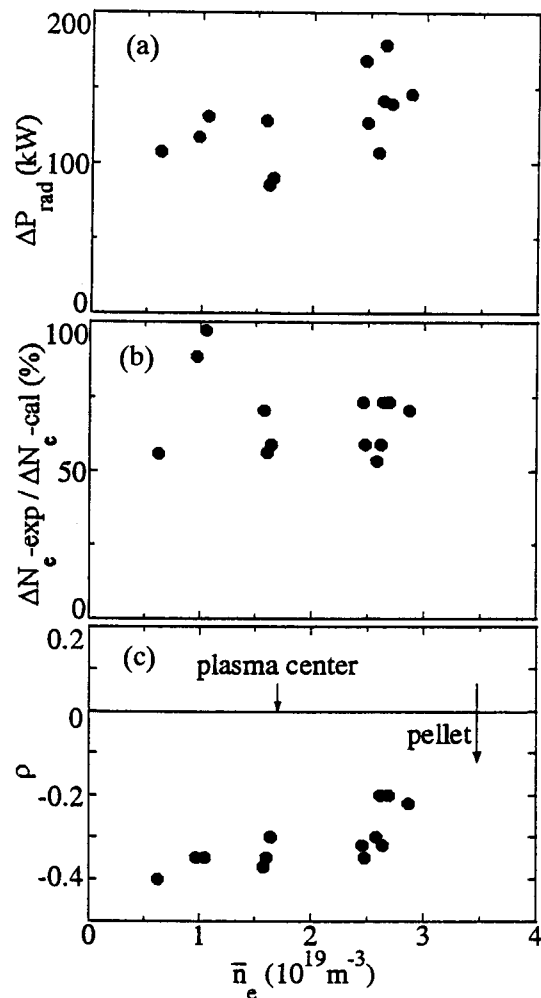


Fig. 3 Increment of the radiation loss (a), fueling efficiency (b) and radial position where the pellet penetrated (c) after pellet ($\phi = 0.30$ mm) injection as a function of the line-averaged electron density of the target plasma before pellet injection.

assumed that the carbon atoms are fully ionized in the plasma. The scattering of the ratio is mainly due to the uncertainty of the edge density profile. From the array measurement it is confirmed that all the pellet are completely ablated. However, there is a tendency that the ratio of $\Delta N_e\text{-exp}/\Delta N_e\text{-cal}$ decreases below 1.0 with increasing pellet size. It seems that the decrease of the ratio is caused by the decrease of the charge state of the injected carbon ions due to the drop of the electron temperature. Figure 3 shows that the increment of the radiation loss (a), fueling efficiency (b) and the radial position of pellet penetration (c) are plotted against the line-averaged electron density in the case of pellet diameter of 0.30 mm. The radiation loss slightly

increases for increasing target density. The fueling efficiency is roughly 70%. The injected pellet reaches the inboard side beyond the plasma axis.

A typical result for the hydrocarbon pellet (0.27 mm ϕ) injection is shown in Fig. 4. In the case of NBI ($P_{\text{NBI}} = 900$ kW), the pellet is injected at $t = 115$ ms for the low-density target plasma ($n_e = 1 \times 10^{19}$ m $^{-3}$). The density increment $\Delta \bar{n}_e$ is 3.1×10^{18} m $^{-3}$. After the pellet injection the central-chord density is gradually increasing until the end of the NBI pulse, whereas the edge density ($\rho = 0.7$) slightly decreases. In the case of ECH ($f_{\text{ECH}} = 53$ GHz, $P_{\text{ECH}} = 200$ kW), the pellet is also injected for the same target density as the NBI case. The central-chord density after the pellet injection is kept constant, whereas the edge density ($\rho = 0.7$)

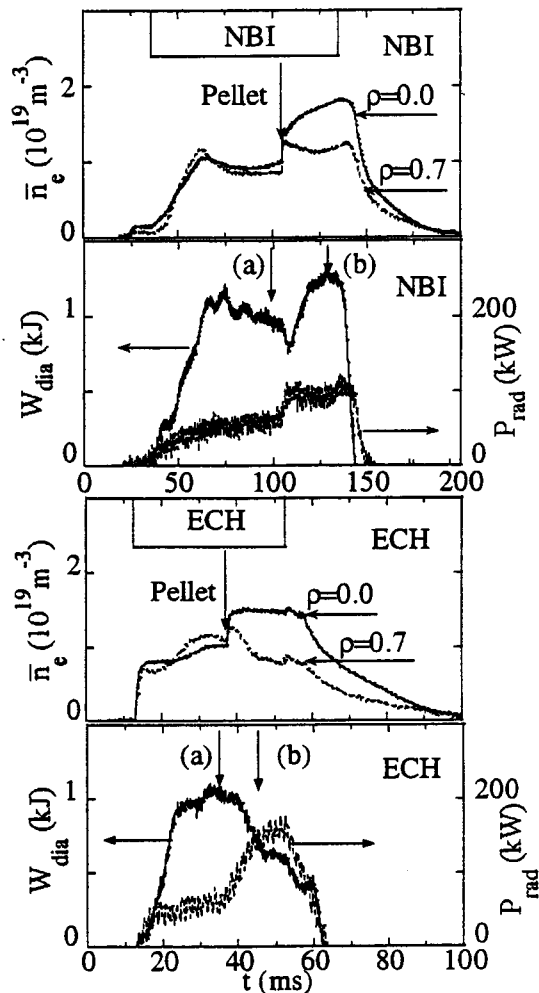


Fig. 4 Time evolution of line-averaged density, plasma stored energy (solid line) and radiation loss (dashed line) with hydrocarbon pellet ($\phi = 0.27$ mm) injection. Vertical arrows (a) and (b) indicate a timing of Thomson scattering measurement ($P_{\text{NBI}} = 900$ kW).

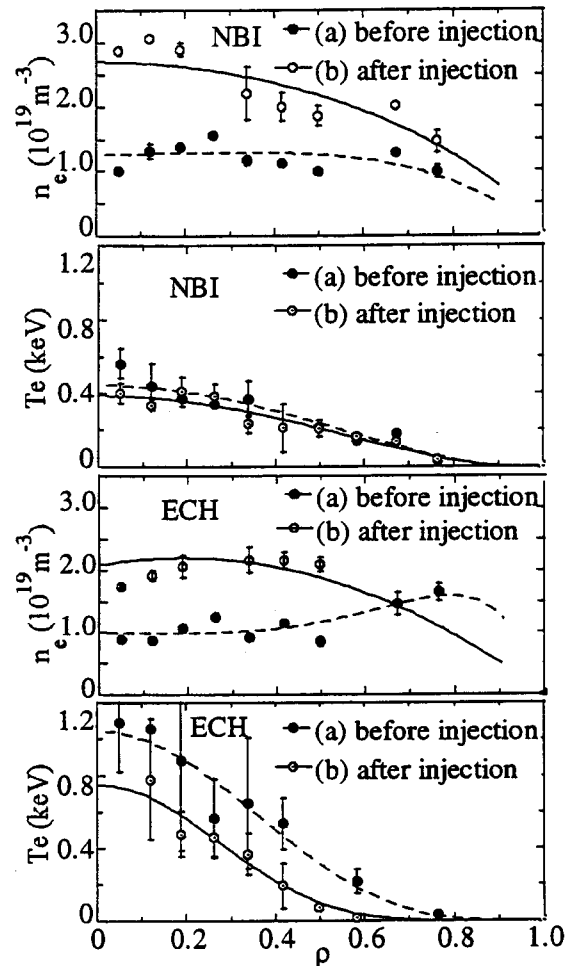


Fig. 5 Profiles of the electron density and temperature before (closed circles) and after (open circles) hydrocarbon pellet ($\phi = 0.27$ mm) injection in NBI and ECH plasmas.

drops largely. In the case of ECH, the edge temperature gradually decreases after the pellet injection. According to the edge temperature drop, the radiation increases until the end of the ECH pulse.

The electron density and temperature profiles before ((a) in Fig. 4) and after ((b) in Fig. 4) pellet injection are shown in Fig. 5. It is clearly seen that after pellet injection the electron density profiles change from flat and hollow profiles to peaked profiles for both cases in the NBI and ECH plasmas. The injected pellet is mainly ablated in the plasma center for both cases. The peaked profile is kept until the end of the heating pulse (also see Fig. 4). This indicates that the particle confinement in the plasma center is very long compared with the edge particle confinement time τ_p , typically 2–5 ms [4], and at least it has a value more than 20 ms. On the contrary, the density behavior in the outer region of the ECH plasma is entirely contrastive in comparison with the NBI plasma. The peak of the density profile at $\rho = 0.8$ is disappeared after pellet injection, whereas in case of the NBI plasma the density at the same position increases. It seems that these results indicate an importance of the source term on the mechanism of the density profile formation. The further experiment will be made under considerations of the superthermal electron behavior and magnetic configurations.

4. Conclusion

The plasma response after hydrocarbon pellet injection with various sizes were studied in the NBI and ECH discharges of CHS. The stored energy increased for the pellet with a diameter smaller than 0.32 mm in the NBI plasma ($P_{\text{NBI}} = 900$ kW, $P_{\text{rad}}/P_{\text{NBI}} = 0.18$). It was observed that in the ECH plasma the electron density profile clearly changed from the hollow profile to the peaked profile after hydrocarbon pellet injection. The peaked density profile was maintained until the end of the heating pulse. These results demonstrated that the impurity pellet is enough applicable to the study of the plasma particle transport.

Reference

- [1] A. Iiyoshi *et al.*, *Fusion Technology* **17**, 169 (1990).
- [2] K. H. Behringer *et al.*, *Nucl. Fusion* **29**, 415 (1989).
- [3] S. Morita *et al.*, *Nucl. Fusion* **30**, 938 (1990).
- [4] S. Morita *et al.*, *Fusion Technology* **27**, 239 (1995).